07,08

Connected structural and ferroelectric phase transitions in perovskites in terms of the deformation order parameters

© L.S. Metlov, M.M. Gordei, Yu.D. Zavorotnev, V.N. Varyukhin

Galkin Donetsk Institute for Physics and Engineering,
Donetsk, Russia

E-mail: lsmet@donfti.ru

Received July 28, 2024
Revised January 31, 2025
Accepted February 1, 2025

Based on Landau's phenomenological theory, the patterns of coupled structural and ferroelectric phase transitions in alloys prone to tetragonal distortions have been investigated. Through numerical experiments, it has been demonstrated that the presence of a weak coupling between the ferroelectric and structural subsystems, provided that the critical temperature of the ferroelectric transition is above the critical temperature of the structural phase transition, will induce weak tetragonal lattice distortions in the interval between the critical temperatures. As the level of coupling increases, the critical temperatures of both transitions converge and may ultimately coincide in the limit.

Keywords: ferroelectric phase transitions, structural phase transitions, order parameter, critical temperatures, weak tetragonal phase.

DOI: 10.61011/PSS.2025.02.60684.201

1. Introduction

It is known that ferroelectric phase transitions are invariably accompanied by structural phase changes. For example, in the $BaTiO_3$ perovskite compound, these are successive transitions to tetragonal, orthorhombic and rhombohedral phases [1–3]. At the same time, structural phase transitions may be followed by phase transitions in magnetic [4–6] and electronic [3] subsystems.

Landau's thermodynamic theory for ferroelectric phase transitions was first proposed by Ginzburg [7–9]. An electric polarization vector was chosen as the order parameter for conventional (intrinsic) ferroelectrics, the second and fourth degrees of polarization modulus P were included in the thermodynamic potential

$$\Phi = \Phi_0 + \frac{\alpha}{2} P^2 + \frac{\beta}{4} P^4 + \dots . \qquad (1)$$

Here, α and β depend on temperature and pressure. According to (1), Ginzburg assumed that second-order or first-order, approximated to the second order, phase transitions might undergo in some ferroelectrics, for example, in triglycine sulfate [10].

With order parameter selection, electric moment was oriented randomly and didn't take into account the crystal anisotropy. Additionally, most of ferroelectrics undergo first-order phase transitions. In 1949, Devonshire proposed a more adequate model, where free energy included two second-degree and fourth-degree invariants and one of the sixth-degree invariants of the three-component order parameter [11]

$$\Phi = \Phi_0 + \frac{1}{2}\chi(P_x^2 + P_y^2 + P_z^2) + \frac{1}{4}\xi_{11}(P_x^4 + P_y^4 + P_z^4) + \frac{1}{2}\xi_{12}(P_x^2P_y^2 + P_y^2P_z^2 + P_z^2P_x^2) + \frac{1}{6}\xi(P_x^6 + P_y^6 + P_z^6). \qquad (2)$$

Free energy of such format gives four types of stable solutions with zero polarization and with polarization vector directed along the center of one of the lattice cell cube sides [100], parallel to the cube face diagonal [110] and along the main cube diagonal [111]. It is naturally to correlate the polarization along one of the cube sides with tetragonal distortions of the cubic structure, though such possibility was not explicitly addressed in studies conducted in this field [7–9,12–14].

To explain the whole chain of ferroelectric phase transitions in $BaTiO_3$, more complex Landau free energy configurations were proposed later, including many invariants for polarization vector components [15–17]. In [15], free energy was postulated by the sixth-degree polynomial where three coefficients depended critically on temperature. In [16,17], it was addressed in the form of 8-th degree polynomials.

Indenbom pointed out that, since the ferroelectric transition was virtually always followed by lattice distortion, then one order parameter in the form of an electric polarization vector was not sufficient and order parameters describing structural changes should be considered [18,19]. To describe phase transitions in extrinsic ferroelectrics within a theory with a two-component microscopic structural order parameter, numerous thermodynamic potentials were proposed that differed from each other in a set of invariants, but two types

of potentials are sufficient to cover the existing experimental data [13,20–22]

$$\Phi = \Phi_0 + \frac{\alpha}{2}(\eta^2+\xi^2) + \frac{\beta_1'}{4}(2\eta\xi)^2 + \frac{\beta_2'}{4}(\eta^2-\xi^2)^2 + \frac{\gamma}{6}(\eta^2+\xi^2)^3 + \frac{\delta}{8}(2\eta\xi)^4, \quad (3)$$

$$\Phi = \Phi_0 + \frac{\alpha}{2}(\eta^2+\xi^2) + \frac{\beta_1'}{4}(2\eta\xi)^2 + \frac{\beta_2'}{4}(\eta^2-\xi^2)^2 + \frac{\beta_3'}{4}2\eta\xi(\eta^2-\xi^2) + \frac{\gamma}{6}(\eta^2+\xi^2)^3. \quad (4)$$

Here, the order parameter components η and ξ are a combination of atom migration in a lattice cell. Note that extrinsic ferroelectric polarization in this model is the second-order infinitesimal effect [13].

Combined consideration of the microscopic structural order parameter η and electric moment P [23,24]

$$\Phi = \frac{1}{2}\alpha_1\eta^2 + \frac{1}{4}\beta_1\eta^4 + \frac{1}{2}\alpha_2P^2 + \frac{1}{4}\beta_2P^4 + \frac{1}{2}\gamma\eta^2P^2 - PE, \quad (5)$$

where E is the external electric field strength, or [20]

$$\Phi = \Phi_0 + \frac{\alpha}{2}\eta^2 + \frac{\beta}{4}\eta^4 + \frac{\gamma}{6}\eta^6 + \frac{\kappa}{2}P^2 + \frac{a}{2}\eta^2P^2 - PE, \quad (6)$$

makes it possible to take into account simultaneously the loss of stability of the structural and ferroelectric subsystem, and their cross-effect due to subsystem interaction (the last but one term).

For intrinsic ferroelectrics, structural lattice distortions, though to a smaller extent, but also might affect the form and parameters of the ferroelectric phase transition through a trigger effect [21]. Phase transitions in systems with related order parameters of different nature may be generally assumed [22–34]. Unlike the above-mentioned works that use the microscopic structural order parameter, this work formulates the theory in terms of a deformational order parameter.

2. Theoretical

The idea of this work is in describing the polarization effects in ferroelectrics using the macroscopic deformational order parameter $\varepsilon_{\alpha\beta}$, where α and β are the Cartesian components of the deformation tensor. The deformational order parameter may be used to describe the variation of many physical properties in PT (phase transition), but low-symmetry phase errors are possible [35]. However, in our case, the type of low-symmetry phase is not determined, but the qualitative picture of PT (phase transition) is examined.

Free energy density for tetragonal distortion cases during structural transition similarly to [4–6] may be written as

$$f = f_0 + \frac{1}{2}a(e_2^2+e_3^2) + \frac{1}{3}be_3(e_3^2-3e_2^2) + \frac{1}{4}c(e_2^2+e_3^2)^2 + \frac{1}{2}a_EP^2 + \frac{1}{4}b_EP^4 + D_2\left(\frac{1}{\sqrt{2}}e_2(P_1^2-P_2^2) + \frac{1}{\sqrt{6}}e_3(3P_3^2-P^2)\right), \quad (7)$$

where a, b, c are the linear combinations of the second-order, third-order and fourth-order elastic constants of the structural subsystem, a_E, b_E are the temperature-dependent constants of the ferroelectric subsystem, D_2 is the parameter responsible for subsystem interaction. Hereinafter, P_1, P_2, P_3 are thex, y, z components of material polarization, P is the polarization modulus, e_2, e_3 are the linear combinations of the Cartesian components of deformation tensor

$$e_1 = (e_{xx}+e_{yy}+e_{zz})/\sqrt{3}, \quad e_2 = (e_{xx}-e_{yy})/\sqrt{2}, \quad e_3 = (2e_{zz}-e_{xx}-e_{yy})/\sqrt{6}. \quad (8)$$

For the purpose of our review, it is assumed that the critical dependence on temperature takes place only through coefficients of quadratic invariants

$$a = a_0(T-T_S), \quad \alpha = \alpha_0(T-T_C), \quad (9)$$

where a_0, α_0 are some new constants, T_S is the critical temperature of structural transition, T_C is the Curie temperature.

Structural component of the free energy density in variables e_2, e_3 is typical for crystals undergoing tetragonal distortions in phase transition [4–6,36]. Ferroelectric component of free energy density corresponds to classical concepts and was borrowed from [7,8]. This work will be limited to the highest contribution of the fourth degree of single-component ferroelectric order parameter P^4 implying that the ferroelectric subsystem on its own can make the second-order phase transition [10]. However, we'll show below that due to the trigger interaction with the structural subsystem, this transition may become similar to the first-order phase transition.

Note that consideration of the sixth degree P^6 makes sense only when b_E of the fourth degree is negative. This may be realized at some critical dependence of this coefficient on temperature similar to (8) or due to interaction with the structural subsystem through the mixed 5-th degree invariants, which is not included in model (7).

The last term in the free energy density proportional to D_2 describes the interaction between structural and ferroelectric subsystems and is also invariant with respect to rotations at angles $\pm 2\pi/3$ of the three-fold axis coinciding with the main diagonal of the lattice cell cube and is written similarly to the magnetic materials [4–6]. Such analogy is quite acceptable directly for order–disorder

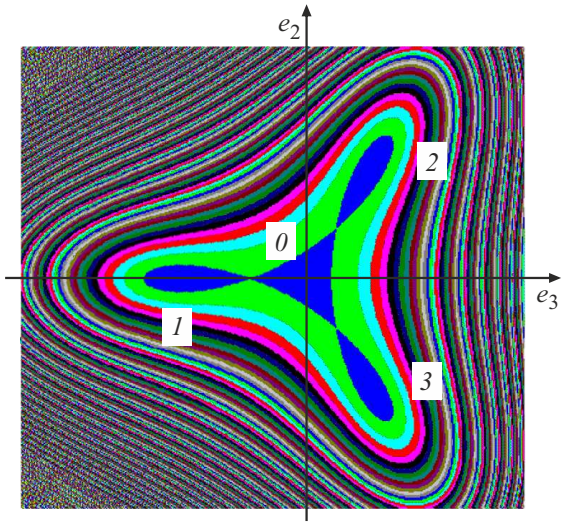

Figure 1. Free energy density isolines on plane e_3-e_2 at $T_{eq} = 155\,\mathrm{K}$ [39]. (Conceptual picture).

ferroelectrics [37,38], coincidence of critical temperatures T_S and T_C is probably required additionally for displacement-type ferroelectrics [37,38].

The presence of three-fold axes coinciding with the main diagonals of the cube leads to the fact that isolines of the structural component of free energy density in (7) on plane e_3-e_2 outline three minima *1–3* (Figure 1) corresponding to the stable existence of three low-symmetry phase options [39]. In the center of the plane, there is also minimum *0* corresponding to the stable state of high-symmetry phase. It is easy to show that minima *1, 2, 3* in Figure 1 correspond to the deformation of lattice cell cube along the z, y, x coordinates, respectively, i. e. coincide with the four-fold axes.

Equilibrium values of order parameters can be found from the system of equations

$$\frac{\partial\Phi}{\partial e_2} = e_2[a - 2be_3 + c(e_2^2 + e_3^2)] + D_2\frac{1}{\sqrt{2}}(P_1^2 - P_2^2) = 0, \tag{10a}$$

$$\frac{\partial\Phi}{\partial e_3} = e_3[a + be_3 + c(e_2^2 + e_3^2)] + D_2\frac{1}{\sqrt{6}}(3P_3^2 - P^2) = 0, \tag{10b}$$

$$\frac{\partial\Phi}{\partial P_1} = P_1\left(a_E + b_E P^2 + c_E P^4 + D_2\left(\sqrt{2}e_2 - \sqrt{\frac{2}{3}}e_3\right)\right) = 0, \tag{10c}$$

$$\frac{\partial\Phi}{\partial P_2} = P_2\left(a_E + b_E P^2 + c_E P^4 - D_2\left(\sqrt{2}e_2 + \sqrt{\frac{2}{3}}e_3\right)\right) = 0, \tag{10d}$$

$$\frac{\partial\Phi}{\partial P_3} = P_3\left(a_E + b_E P^2 + c_E P^4 + 2\sqrt{\frac{2}{3}}D_2 e_3\right) = 0. \tag{10e}$$

Depending on the relation of constants, the ferroelectric subsystem (intrinsic ferroelectrics) or structural subsystem (extrinsic ferroelectrics) might prevail in model (7)–(9). Besides the power parameters of the model, relation between T_C and T_S can also affect the form of subsystem interaction. When $T_C > T_S$, then the ferroelectric phase transition occurs earlier during cooling, due to which non-zero components of P_i will have a higher impact on the structural subsystem than on the opposite case. In this case, an intrinsic ferroelectric will be realized. In case of an opposite inequality $T_C < T_S$, an extrinsic ferroelectric will be realized.

3. Change of electric moment polarization

It is difficult to solve system of equations (10) analytically. Therefore, it was examined by numerical methods with the following values: $a_{E0} = 1$, $b_E = 1$, $a_0 = 0.7$, $b = 0.333$, $c = 1$, $D_2 = 0.02$, $T_S = T_C = 150\,\mathrm{K}$. Equality of T_S and T_E was assumed based on the hypothesis that both types of phase transitions, structural and ferroelectric, can occur only simultaneously, rather than separately. Relaxation of the order parameters η_k obey the system of the Landau–Khalatnikov evolution equations [39]:

$$\frac{\partial\eta_k}{\partial t} = -\gamma_k\frac{\partial\Phi}{\partial\eta_k} + f_k(\eta_k), \tag{11}$$

where η_k is the variable corresponding for indices $1, 2, 3$ to the ferroelectric order parameter components P_1, P_2, P_3, and for indices $4, 5$ to the structural components e_2, e_3, γ_k — kinetic coefficients, $f_k(\eta_k)$ — function simulating thermal fluctuations or noise in the form of white noise.

We choose the initial temperature a little lower than the critical point 150 K, so that the initial values of the order parameter components are equal to $P_1 = P_2 = P_3 = 0.0001$, $e_2 = 0.005$, $e_3 = -0.05$, i. e. the system is in the region of attraction to minimum *1* on the free energy density profile (Figure 1), and the system is placed in a thermostat at 140 K (overcooling 10 K). For deformational order parameters, relaxation to the new equilibrium state undergoes monotonously and stops at $e_2 = 0$ and $e_3 = -0.507$ (curves *4, 5*, Figure 2).

Electric moment relaxation takes place according to a qualitatively different scenario. There is a time point t_{cr}, denoted with line AB in Figure 2, such that at $t < t_{cr}$ all three polarization vector components grow, while the vector itself is directed along the three-fold axis (main diagonal of the lattice cell cube). A weak tetragonal distortion occurs already in the structural subsystem (curve *5*, Figure 2), however, it is small and cannot change the polarization vector orientation essentially. With $t > t_{cr}$, tetragonal distortion in the structural subsystem grows drastically (curve *5*, Figure 2) and leads to the decrease in P_2, P_3 to zero and to the growth of P_1 reaching some asymptotic value (curves *1–3*, Figure 2). Such behavior indicates that the vector rotates from the three-fold axis to the four-fold axis of the tetragonal phase.

A brief conclusion may be made that, regardless of the selected region of attraction to a particular minimum at certain structural distortions, there is a jump of electric moment vector direction from the three-fold axis to the fourth-fold axis of the tetragonal phase. Different attraction regions correspond to the jumps to different fourth-fold axes [39].

For comparison, the inset in Figure 2 shows the plot of the kinetics of P_i for the real $BaTiO_3$ compound calculated according to (11) using the intrinsic ferroelectric model (without considering the structural subsystem) with the Gibbs free energy and parameters borrowed from Table 1 in [15]. Calculation is limited to the tetragonal phase existence region with freezing depth at $T_c = 393$ K. As can be seen, the polarization vector rotation effect in the material relaxation process also takes place here.

4. Hysteresis phenomena

Relaxation of some material in isothermal conditions at $T = 140\,\mathrm{K} < T_S$ was discussed above. To investigate potential hysteresis phenomena, it is interesting to examine the behavior of the same material without a thermostat at the initial temperature of 160 K with constant cooling and heating rate (Figure 3).

Since the initial temperature is higher than the structural phase transition temperature $T = 160\,\mathrm{K} > T_S$, then the material restores its cubic symmetry at the initial cooling stage with all order parameters equal to zero. Structural transition at this cooling rate really goes at approx. 140 K (curves *4, 5*, Figure 3). It also induces ferroelectric transition (kcurves *1–3*) according to a scenario described in 2, i. e. with rotation of the polarization vector from the three-fold axis to the fourth-fold axis [40].

P_3 decreases monotonously as the temperature grows during heating, thus, demonstrating the hysteresis (upper branch of curve *3*, Figure 3). The degree of tetragonal distortion decreases at the same time, also demonstrating the hysteresis (lower branch of curve *5*). Note that the structural phase transition with and without considering the polarization subsystem is a first-order transition with the typical hysteresis. At the same time, when the interaction of two subsystems is considered, the polarization subsystem behavior changes significantly, the order of phase transition changes and the temperature hysteresis occurs.

Note also that the reverse phase transition with respect to the electric moment (curves *1–3*, Figure 3) to the high-symmetry phase with zero order parameter is completed earlier than the structural phase transition itself (at $\sim$ 153 and 160 K).

5. Kinetics of spontaneous electric moments at $T_C > T_S$

Assume the Curie temperature for the electric subsystem T_C is higher than the critical temperature of structural

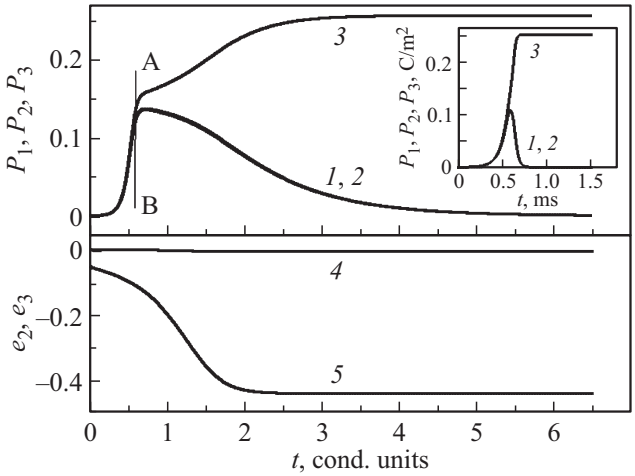

Figure 2. Time relaxation of the order parameters from the initial state with attraction to minimum *1* at 140 K. Initial values $P_1 = P_2 = P_3 = 0.0001$, $e_2 = 0.005$, $e_3 = -0.05$. Here, *1, 2, 3* — electric moment components; *4, 5* — deformational order parameters e_2 and e_3. The inset shows the model and parameter calculation from [15].

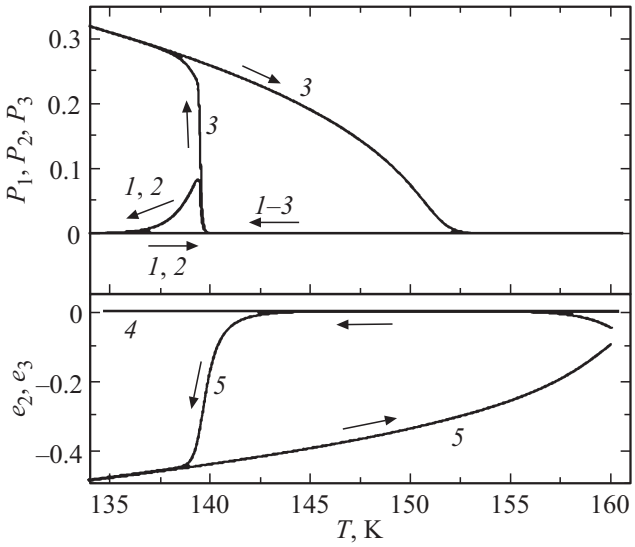

Figure 3. Temperature hysteresis of the order parameters during cooling and heating at a rate of 1 K/cond.units. Designations are the same as in Figure 2.

transition T_S, for example, $T_S = 150$ K, $T_C = 175$ K with the same remaining parameters. Order parameter relaxation in this case has generally the same form as that for coinciding critical temperatures, but there are quantitative differences (Figure 4). It can be seen that the equilibrium state in time, when the critical temperatures don't coincide, is achieved with a higher rate and the curves move to the left. Hence, it follows that the electric vector component behavior varies in an earlier time interval and at higher deformation module. Equilibrium values of the order parameters increase in

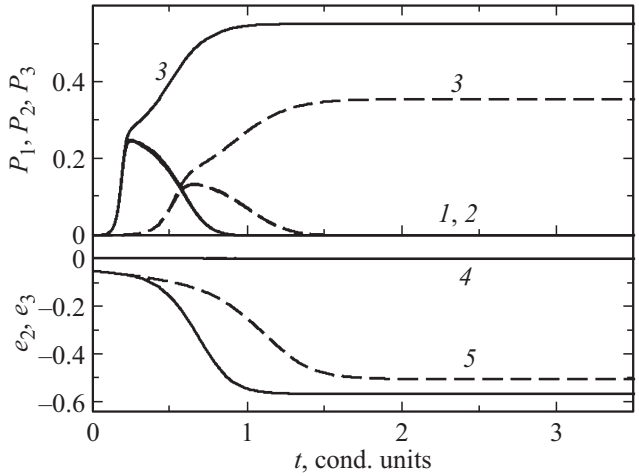

Figure 4. Order parameter relaxation at the thermostat temperature $T = 140\,\mathrm{K}$ at various critical temperatures $T_S = 150\,\mathrm{K}$, $T_C = 175\,\mathrm{K}$, (solid lines) and $T_S = T_C = 150\,\mathrm{K}$ (dashed lines). Designations are the same as in Figure 2.

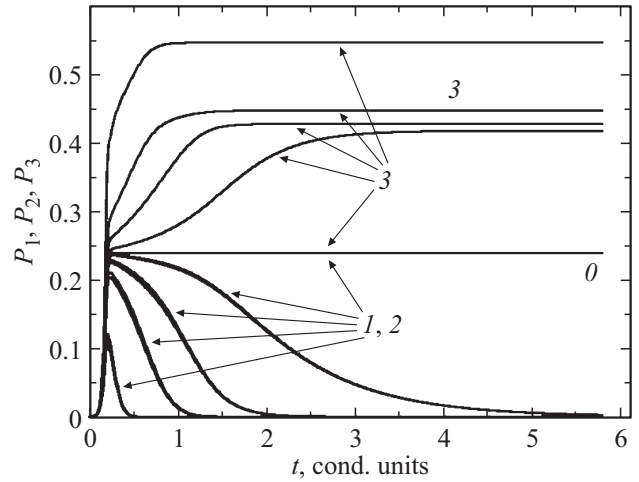

Figure 5. Relaxation of spontaneous electric moment components at $T = 140\,\mathrm{K}$ at various interaction levels: $D_2 = 0$, 0.005, 0.02, 0.05, 0.2, for $T_S = T_C = 150\,\mathrm{K}$. Designations are the same as in Figure 2.

absolute magnitude (curves *3, 5*), and, consequently, the slope of corresponding curves grows in the transition region.

Phase transition kinetics of the electric and structural subsystems at some fixed level of interaction between them $D_2 = 0.02$ was discussed above. It is interesting to address the effect of D_2 on the form of phase transitions individually.

6. Effect of the subsystem interaction level

We examine the behavior of curves describing the above-mentioned phase transition at 140 K and $D_2 = 0$, 0.005, 0.02, 0.05, 0.2. Figure 5 shows the ferroelectric vector component kinetics for these cases. At $D_2 = 0$ (hypothetical case), there is no interaction between subsystems and each transition occurs individually, i. e.occurrence of tetragonality in the structural subsystem doesn't affect the moment vector module and direction in any way. Therefore, the system almost immediately changes to the stationary state. This trend is shown by straight line No.0 and corresponds to purely ferroelectric transition, which is indicative of a constant electric vector direction along the three-fold axis of the cube and of the absence of the polarization change effect.

Increase in D_2 gives rise to the increase in mutual influence of subsystems. As shown in Figure 5, increase in the module of vector directed along the three-fold axis in initial times depends weakly on D_2. Then, transition to the stationary state starts almost simultaneously. Behavior of this transition depends considerably on D_2. The higher D_2 the quicker the stationary state is achieved with the polarization vector rotation along the fourth-fold axis of the tetragonal phase. As D_2 decreases, the inflection points of curves P_1, P_2, P_3 shift to the right, which indicates that equilibrium is achieved at a later time.

7. Low tetragonality and shift of the critical temperature of structural transition

Temporary relaxation of transition to the final state was examined in the previous section on the assumption that two subsystem temperatures coincided. However, time trend variation should be expected at various critical temperatures (for example, at $T_C = 175\,\mathrm{K}$ and $T_S = 150\,\mathrm{K}$). In this case, a forced structural phase transition takes place under the influence of a higher temperature ferroelectric transition. It is interesting to study the temperature process of variation of the structural order parameter at such phase transition (Figure 6).

For earlier induction of the phase transition, equation (10) took into account thermal fluctuations or noise. As shown in Figure 1, all existing low-symmetry phase options are equivalent. We assume that the system has randomly selected the 3-rd low-symmetry phase option as a result of fluctuations during temperature reduction. As a consequence, in this case $e_3 > 0$, $e_2 < 0$.

As specified above, when subsystem interaction is absent or low, the structural transition is spontaneous and is characterized by quick changes of the order parameter, i. e. the corresponding curves in the phase transition region have the maximum first-order derivatives in absolute magnitude (segment BC in Figure 6). It can be seen that the transition temperature region becomes smoother with the growth of interaction, which is due to the effect of the non-zero polarization vector.

With the highest D_2, the corresponding curves get smoothed insomuch that the order of forced phase transition actually changes from the first to the second one. This

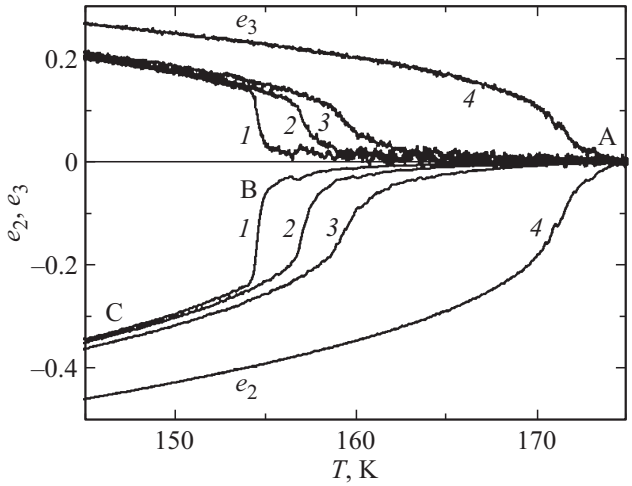

Figure 6. Temperature dependences of e_2, e_3 during cooling at a rate of 1 K/cond.units. on $T = 176$ K for $T_C = 175$ K, $T_S = 150$ K. The curves are numbered in the order of increasing D_2: *1* — 0.01, *2* — 0.02, *3* — 0.04, *4* — 0.2.

change features the increase in temperature of the critical point of structural phase transition approximately to 168 K. In view of the foregoing, it can be suggested (to be verified in future) that, as the interaction of two subsystems D_2 grows, the temperatures of both phase transitions converge and coincide at the limit.

Finally, note that a weak tetragonality may be used as a small parameter. In this case, leaving the lowest degree of the structural order parameter in (10 a,b), we express e_2 and e_3 in terms of the polarization order parameters

$$e_2 = -\frac{D_2}{a}\frac{1}{\sqrt{2}}(P_1^2 - P_2^2), \quad e_3 = -\frac{D_2}{a}\frac{1}{\sqrt{6}}(2P_3^2 - P_1^2 - P_2^2). \tag{12}$$

Free energy density (7) in this case rearranges to

$$\Phi = \Phi_0 - \frac{D_2^2}{a}(P_1^4 + P_2^4 + P_3^4 - P_1^2P_2^2 - P_1^2P_3^2 - P_2^2P_3^2) + \frac{1}{2}a_E P^2 + \frac{1}{4}b_E P^4. \tag{13}$$

Except the highest degree of the order parameter, equation (13) coincides with the Devonshire equation (2), if the following is set

$$\xi_{11} = 4\left(b_E - \frac{D_2^2}{a}\right), \quad \xi_{12} = b_E + 2\frac{D_2^2}{a}. \tag{14}$$

Negative values of ξ_{11} at all positive remaining coefficients correspond to the stable existence of the tetragonal phase [11].

Thus, the phase transitions in intrinsic ferroelectrics may be described in terms of electric polarization without any prejudice. The related variations of lattice symmetry and deformation in this case are the second-order infinitesimal effect and might be expressed explicitly as (12) (see also equations (9.6) in [11]).

8. Conclusion

Thus, in terms of deformational and electric order parameters, a theory of phase transitions in the structural and ferroelectric subsystems was developed, with one of the phase transitions being forced due to the interaction. The theory refers to materials that undergo tetragonal distortions in such transitions.

Stepwise variation of the electric polarization direction was found at the initial system relaxation stage from the three-fold axis to the fourth-fold axis direction. This effect increases as the critical temperature difference between the proper ferroelectric transition and structural transition grows. At a low interaction constant D_2, both transitions take place in different times. Electric transitions is the main one and causes forced weak distortions of the structural subsystems.

At higher D_2, the structural transition is smeared and the transition temperature interval grows. It may be expected that in the limit of very strong interactions, the temperatures of both phase transitions will coincide, and the form of phase transition will change from the first to almost the second one.

During cyclic cooling-heating, the hysteresis phenomenon was detected, both with respect to the structural and electric order parameter. It is shown that the stepwise electric moment polarization change effect takes place only at the material cooling stage. Whereas during heating, the electric moment retains the polarization along the fourth-fold axis and smoothly vanishes at high temperatures. It is also shown that, during cooling, the time of polarization jump from the main diagonal direction to the direction of one of the lattice cell cube sides is inversely proportional to D_2.

Conflict of interest

The authors declare no conflict of interest.

Funding

The work was performed under the publicly funded research and development project „Formation of the Structure and Properties of Promising Multifuctional Materials“ (2019–2025).

References

[1] A.E. Panich, T.G. Levina. Fizika segnetoelekticheskoi keramiki. Ministerstvo obrazovaniya RF, Rostovsky gosudarstvenny universitet, Rostov-na-Donu (2002). 45 s. (in Russian).
[2] O.S. Sirotkin, T.B. Tatarintseva, I.A. Zhenzhurist. Provodnikovye, poluprovodnikovye, dielektricheskie i magnitnye materialy: uchebnoe posobie. Kazansky gosudarstvenny energetichesky universitet, Kazan (2017). 352 s. (in Russian).
[3] S.G. Dzhabarov. Uspekhi fiz. mat., **329**, 2015 (2013). (in Russian).

[4] A.N. Vasil'ev, A.D. Bozhko, V.V. Khovailo, I.E. Dikshtein, V.G. Shavrov, V.D. Buchelnikov, M. Matsumoto, S. Suzuki, T. Takagi, J. Tani.Phys. Rev. B **59**, 1113 (1999).
[5] A.D. Bozhko, A.N. Vasiliev, V.V. Khovailo, I.E. Dikshtein, V.V. Koledov, S.M. Seletsky, A.A. Tulaikova, A.A. Tchechukin, V.G. Shavrov, V.D. Buchelnikov. JETP **115**, 1740 (1999). (in Russian).
[6] V.D. Buchelnikov, A.T. Zayak, A.N. Vasiliev, D.L. Dalidovich, V.G. Shavrov, T. Takagi, V.V. Khovailo. ZhETF **119**, *6*, 1166 (2001). (in Russian).
[7] V.D. Ginzburg. ZhETF **15**, 739 (1945). (in Russian).
[8] V.D. Ginzburg. ZhETF **19**, 36 (1949). (in Russian).
[9] V.D. Ginzburg. UFN **38**, *4*, 490(1949). (in Russian).
[10] T.A. Tryukhan, E.V. Stukova, S.V. Baryshnikov. Radiotekhnika i elektronika, **12**, (2010). (in Russian).
[11] A.F. Devonshire. Phil. Mag. **40**, 1040 (1949).
[12] V.D. Ginzburg. UFN **171**, *10*, 1091 (2001). (in Russian).
[13] A.P. Levanyuk, D.G. Sannikov. UFN, **112**, *4*, 561 (1974). (in Russian).
[14] I.S. Rez, Yu.M. Poplavko, Dielektriki. Osnovnye svoistva primeneniya v elektronike. Radio i svyaz, M., (1989). 288 s. (in Russian).
[15] A.J. Bell, L.E. Cross. Ferroelectrics **59**, 197 (1984).
[16] Y.L. Li, L.E. Cross, L.Q. Chen. J. Appl. Phys. **98**, 064101 (2005).
[17] J.J. Wang, P. P. Wu, X. Q. Ma, L. Q. Chen1. J. Appl. Phys. **108**, 114105 (2010).
[18] V.L. Indenbom. Kristallografiya **5**, 115 (1960). (in Russian).
[19] V.L. Indenbom. Izvestiya AN SSSR, ser. Fizicheskaya, **78**, 1960 (2014). (in Russian).
[20] A.P. Levanyuk, D.G. Sannikov. ZhETF **55**, *1*, 256 (1968). (in Russian).
[21] A.P. Levanyuk, D.G. Sannikov. Pisma ZhETF **68**, 1970 (2017). (in Russian).
[22] V. Dvorak. Phys. Stat. Sol. B **46**, 763 (1971).
[23] Yu.M. Gufan, E.S. Larin FTT **22**, *2*, 463 (1980). (in Russian).
[24] E.V. Balashova, A.K. Tagantsev. Phys. Rev. B **48**, *14*, 9979 (1993).
[25] J. Holakovsky. Phys. Status Solidi B **56**, 615 (1973).
[26] M.A. Anisimova, Zh.V. Gorodetsky, V.M. Zaprudsky. UFN **133**, 103 (1981). (in Russian).
[27] A.K. Radzhabov, E.V. Tcharnaya, B. Mroz, C. Tien, Z. Tylczynski, C.-S. Wur. FTT **46**, *4*, 754 (2004). (in Russian).
[28] V.I. Torgashev, V.B. Shirokov, A.S. Prokhorov, L.A. Shuvalov. Crystallogr. Rep. **50**, *4*, 689 (2005).
[29] E.P. Smirnova, A.V. Sotnikov, O.E. Kvyatkovskii, M. Weihnacht, V.V. Lemanov. J. Appl. Phys. **114**, 084116 (2007).
[30] E.V. Balashova, V.V. Lemanov, G.A. Pankova. FTT **49**, *2*, 331 (2007). (in Russian).
[31] P. Toledano, V. Carolus, M. Hudl, Th. Lottermoser, D.D. Khalyavin, S.A. Ivanov, M. Fiebig. Phys. Rev. B **85**, 214439 (2012).
[32] R.G. Burkovsky, A.K. Tagantsev, K. Vaideeswaran, N. Setter, S.B. Vakhrushev, A.V. Filimonov, A. Shaganov, D. Andronikova, A.I. Rudskoy, A.Q.R. Baron, H. Uchiyama, D. Chernikov, Z. Ujma, K. Roleder, A. Majchrowski, Jae-Hyeon Ko. Phys. Rev. B **90**, 144301 (2014).
[33] Ph. Chosez, J. Junquera. Annu. Rev. Condensed Matter Phys. **13**, 325-24 (2022).
[34] S.V. Pavlov. Vestnik Moskovskogo universiteta. **79**, *3*, 2430501 (2024). (in Russian).
[35] Yu.A. Izyumov, V.N. Syromyatnikov. Fazovye perekhody i simmetriya kristallov. Nauka, M. (1984). 247 s. (in Russian).
[36] M.A. Fradkin. Phys. Rev. B **50**, *22*, 326 (1994).
[37] G.A. Smolensky, N.N. Krainik. UFN **97**, *4*, 657 (1969). (in Russian).
[38] V.G. Waks, V.I. Zinenko, V.E. Schneider. UFN **141**, *4*, 629 (1983). (in Russian).
[39] L.S. Metlov, FTVD **33**, *3*, 5 (2023). (in Russian).
[40] L.S. Metlov, FTVD **34**, *1*, 16 (2024). (in Russian).

Translated by E.Ilinskaya